Supplementary Information

Metal-Organic Framework Decorated Whispering-Gallery-Mode Microsphere Cavity for VOCs Sensing

Xianggang Chen,[a]† Xiaoyan Zhang,[a]† Xiaoyi Wu[a,b], Ling Bai*[a] and Yin Yin*[a]

[a]School of Materials Science and Engineering, Jiangsu University, Zhenjiang, Jiangsu Province 212013, China
[b]Institute of Industrial Economics, Jiangsu University, Zhenjiang, Jiangsu Province 212013, China

†The authors contributed equally.

*Corresponding authors.
E-mail addresses: lingmubai@ujs.edu.cn (L.Bai); y.yin@outlook.com (Y.Yin)

Contents

I. Experimental materials

10 mg/ml monodisperse polystyrene(PS) green fluorescent microspheres (with a diameter of ~ 10 μm) were purchased from YUAN BIOTECH; 2-Methylimidazole (2-MIM, 98%), $Zn(NO_3)_2 \cdot 6H_2O$ (analytical purity, AR), and methanol (analytical purity, AR) purchased from Sinopharm Chemical Reagent Co., Ltd; Sodium Dodecyl Sulfate(SDS,AR) was purchased from Sinopharm Chemical Reagent Co., Ltd.; PVP (polyvinyl pyrrolidone, M.W.~40000) purchased from Shanghai Aladdin Biochemical Technology Co., Ltd; Na Ac (sodium acetate, 99% anhydrous) purchased from Heowns Biochem Technologies, LLC, Tianjin; Deionized water(DI water) (made in the laboratory, conductivity < 1 μs/cm)； All reagents used are used as received and have not been further purified.

II. Sample preparation and characterization

Synthesis of ZIF-8 nanoparticles. The synthesis of ZIF-8 nanoparticles is

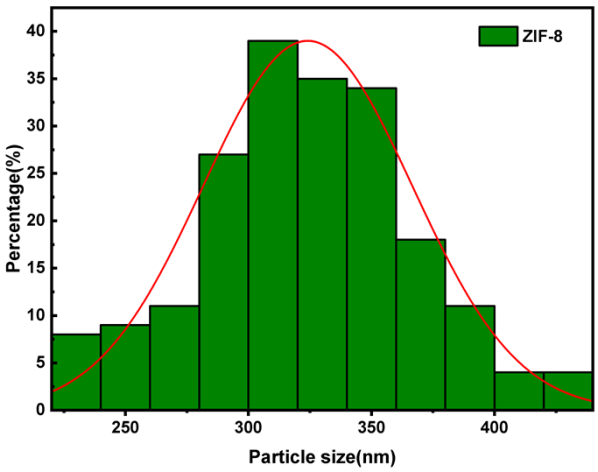

according to previous work [1]. First, 3 mM of 2-MIM and 0.25 g of PVP were dissolved in 50 ml of methanol solution (solution A); 1.5 mM of Zn $(NO_3)_2 \cdot 6H_2O$ was dissolved in 50 ml of methanol solution (solution B); 12 mg of Na Ac was dissolved in 1 ml of methanol solution (solution C). Solution B was quickly added to solution A, and the reaction is accelerated by stirring continuously at room temperature. After the reaction is 10 min, solution C is added to slow down or terminate the reaction. The reaction up to 12 min, it is washed by centrifugation with methanol (8000 r/min, 5 min centrifugation) several times until it is clear.

Figure S1. Particle size distribution of ZIF-8 nanoparticles analyzed by Nano Measurer v1.2.

Self-assembly of ZIF-8 nanoparticles on the surface of the whispering-gallery mode (WGM) microsphere cavity. First, 0.1 ml of the original solution of green fluorescent microspheres were dispersed it in 10 ml of deionized water, configure it into a solution of 1 mg/ml, and store it at 4~10℃ for backup. 25 μl of the configured 1 mg/ml monodisperse polystyrene green fluorescent microspheres (with a diameter of ~ 10 μm) solution were dropped onto the surface of the glass substrate, and dried it naturally. Deionized water and equal volume of absolute ethanol containing ZIF-8 nanoparticles (mass fraction 5.74%) were configured into a solution using, and ultrasonic for several hours to form an evenly dispersed suspension. Secondly, the glass substrate was placed in a petri dish and deionized water is added to make the liquid level higher than the glass substrate. Use a syringe to inject the ZIF-8 nanoparticles

suspension into the gas-liquid interface at a certain speed. After the particles have covered the entire liquid level, an SDS solution with a mass fraction of 2% configured with deionized water was added to the edge of the petri dish. After ten minutes of stabilization, the solution under the ZIF-8 nanoparticles layer in the petri dish was absorbed, and the ZIF-8 nanoparticles layer can be formed on the surface of the PS microspheres cavity after the liquid level drops.

Structural and Compositional Characterizations. The surface morphology of all samples was characterized by field emission scanning electron microscope FEI NovoNano450; the composition of samples were analyzed by smart LAB and a smart multi-function X-ray diffractometer; Use the fully automatic specific surface and pore size distribution analyzer NOVA 3000e for nitrogen absorption-desorption experiments；Under the excitation of a 532 nm laser, the Raman spectrum of the sample was tested on the micro-region Raman and fluorescence measurement system built by the laboratory. The system is composed of a laser, a spectrometer (SpectraPrp HRS-500), a gora-Lite confocal micro-spectroscopy module, an objective lens and other parts. It is notable that the spectrum resolution of the spectrometer (SpectraPro HRS-500, grating: 1800 l/mm) we used to be 0.0056nm, it is therefore capable of precisely detecting the mode shift even with tiny value.

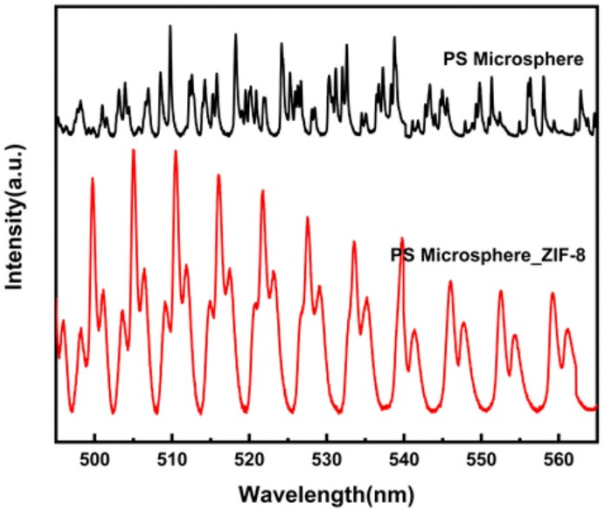

Figure S2. WGMs spectra of PS microsphere cavity before and after ZIF-8-nanoparticle decoration.

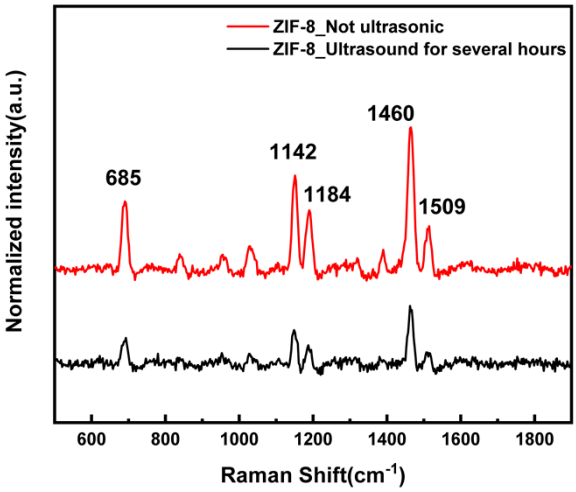

Figure S3. Raman spectra of the ZIF-8 nanoparticles before and after ultrasound

III. Analysis of the Sensing Performance

Experimental Design for Controlling VOC Concentrations. The ethanol gas configuration system with varying concentrations was established by injecting ethanol of corresponding content into a U-shaped tube. The system operated through the following procedure: The U-shaped tube was heated to facilitate ethanol volatilization, while air was introduced through a flowmeter-regulated system (CS200-A) to carry the volatile ethanol gas into a gas collection bag. The schematic diagram of this ethanol gas configuration system with different concentrations was presented in the figure below.

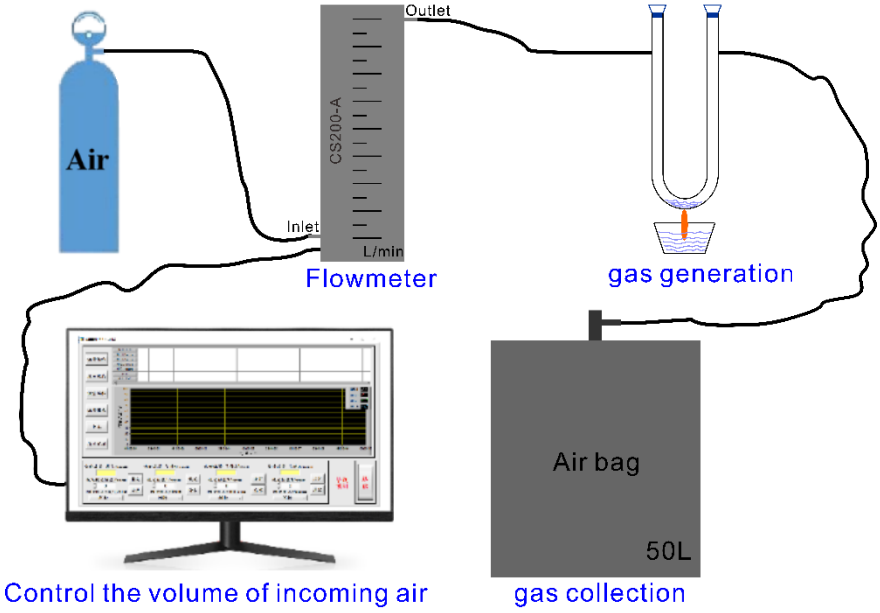

Figure S4. Generation of different concentrations of ethanol gas configuration system

Principles and method for calculating the amount of ethanol. According to the ideal gas law under standard atmosphere, we have:

$$PV = nRT$$

where P is the gas pressure, which is 101.325 kPa at standard atmospheric pressure, and R is the ideal gas constant, which is 8.314 kPa·L/(K·mol), and V, n, and T are the volume of the configuration gas, amount of substance, room temperature, respectively.

In our experiment, V = 30 L, T = 20 ℃, therefore the air to be injected was determined:

$$n_{air} = \frac{PV}{RT} = \frac{101.325kPa \times 30L}{8.314kPa \cdot L/(K \cdot mol) \times (273 + 20)K} = 1.25\ mol$$

For the ethanol gas concentration of 1000 ppm:

$$\frac{n_{gas}}{n_{air}} = 1000 \text{ ppm} = 0.1\% = 10^{-3}$$

Thus,

$$n_{gas} = \frac{PV}{RT} = n_{air} \times 10^{-3} = 1.25 \times 10^{-3}\ mol$$

$$n_{gas} = n_{liquid} = \frac{m_{gas}}{M_{gas}}$$

$$V_{liquid} = \frac{n_{gas} \times M_{gas}}{\rho_{liquid}} = 72.9\ \mu l$$

where n_{air}, n_{gas}, n_{liquid}, m_{gas}, M_{gas}, $V_{liquid,}$ and ρ_{liquid} are the amount of air substance, the amount of ethanol gas substance, the amount of ethanol liquid substance, the mass of ethanol gas, the relative molecular mass of ethanol, the volume of ethanol liquid, and the density of ethanol (0.789g/cm^3), respectively.

Similarly, the amount of liquid required to acquire the concentration of 900 ppm, 1200 ppm, 1500 ppm, 5000 ppm, and 8000 ppm is 65.6 μl, 87.4 μl, 109.3 μl, 364.3 μl, and 582.9 μl, respectively.

Optical measurement system. Using a laser with an excitation wavelength of 405 nm, the optical sensing performance of the sensor in different environments was tested

using the laboratory's self-built micro-region Raman and fluorescence measurement system equipment. The measurement principle is shown in Figure S5. The output laser intensity is 28 mA, equipped with an attenuation sheet of T=5%, the sample was placed in a test chamber with a quartz window, and the flow rate of the gas entering the test chamber is monitored through a flowmeter.

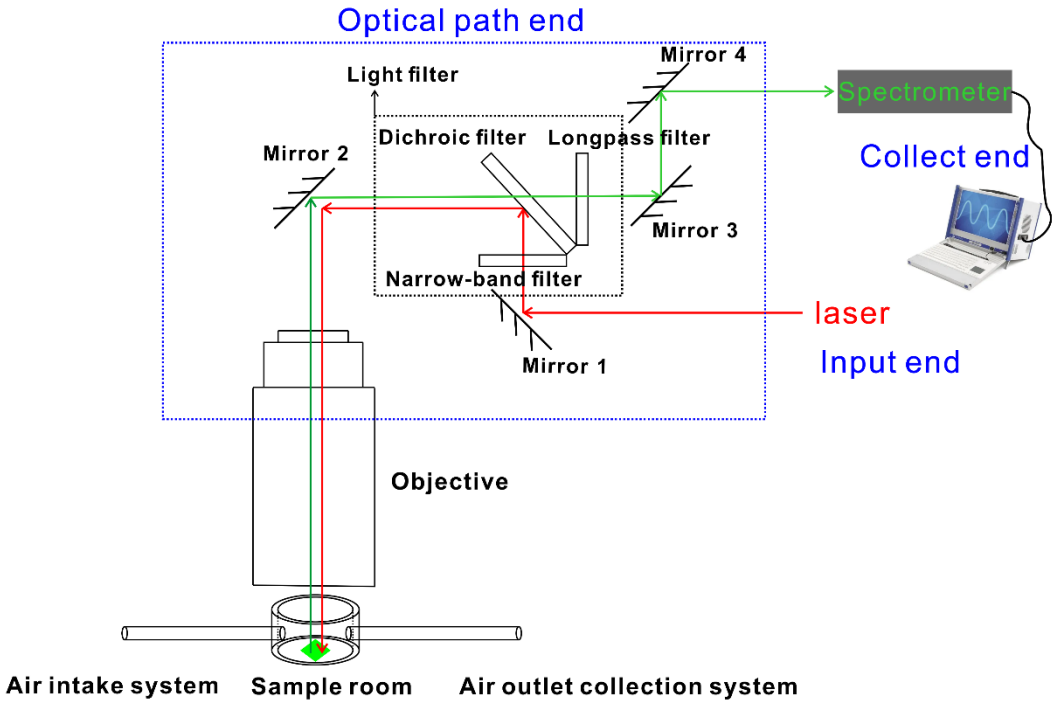

Figure S5. Sketch of the optical measurement system.

Temperature and humidity condition control. The humidity resistance of the sensor was evaluated by introducing deionized water into the U-shaped tube during ethanol gas preparation, enabling the configuration of ethanol gas with varying humidity levels. For the temperature resistance test, infrared lights were used to irradiate the sample chamber, while thermometers monitored real-time temperature changes to establish controlled temperature environments. In both experiments, the sensor was exposed to the target humidity or temperature conditions for a minimum of 10 minutes to ensure stable measurements.

Polystyrene Particle Stability Validation. Since the temperature resistance experiments were conducted within the range of 0–40 °C, well below the glass

transition temperature (Tg) of polystyrene (80–100 °C), the structural integrity and performance of the polystyrene microspheres remained unaffected throughout the testing process. In addition, Polystyrene molecules, which contain non-polar benzene rings, exhibit inherent hydrophobicity. According to a previous study [2], the water adsorption capacity of polystyrene is only 0.5 $mg_{water}/g_{polymer}$ even at a relative humidity (RH) of 80%. This indicates that polystyrene remains largely unaffected by humidity in environments with RH below 80%.

Response characteristics of ZIF-8-nanoparticle decorated microsphere cavities at different ethanol gas concentrations. For the ethanol gas concentration of 8000 ppm, the measurement procedure was conducted as follows. First, the WGM spectrum of the sensor was measured three times in air over a 5-minute interval to establish a baseline. No distinguishable mode shift was observed during this period, confirming the stability of the measurement system. Subsequently, ethanol gas was introduced, and the WGM spectrum was recorded three times at 5-minute intervals. A continuous mode shift was observed during this phase, indicating the sensor's response to ethanol gas. After 10 minutes of exposure to ethanol gas, the spectrum stabilized, and the mode shift remained below the spectral resolution, signifying the saturation of gas adsorption. Finally, air was reintroduced, and the WGM spectrum was measured three times at 5-minute intervals. The spectrum stabilized again after 15 minutes of air exposure. Similar procedures were performed for ethanol gas at other concentrations. The corresponding time-response curve is presented in Figure S6. Based on these experimental observations, the total cycle time was determined to be 40 minutes, consisting of 15 minutes for gas exposure, 10 minutes for response, and 15 minutes for recovery.

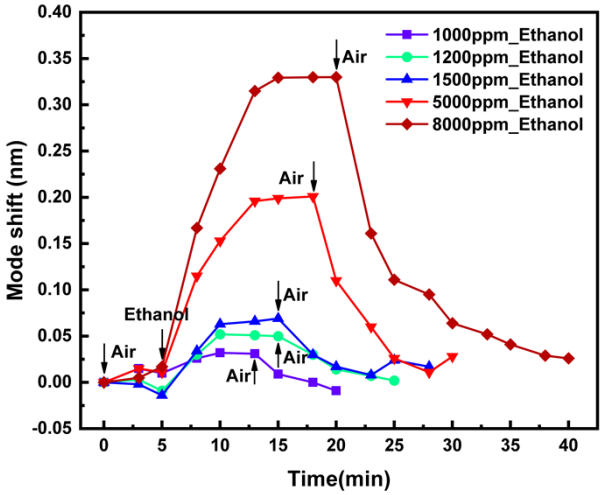

Figure S6. Time response curve of ZIF-8-nanoparticle decorated microsphere cavities at different ethanol gas concentrations.

Calculation of refractive index of ZIF-8 after adsorption of ethanol gas. Firstly, the mode shift varying with the ethanol gas concentration in experiments were derived from Figure S7 (black circle). The linear fitting results yielded the equation:

$$Y=0.0000408\ C-0.00115\ (R^2=0.97)$$

where Y, C, and R^2 are the mode shift, ethanol gas concentration, and correlation coefficient, respectively.

In the simulation, the variation of ethanol gas concentration was replaced by the change in refractive index of ZIF-8. Therefore, to match linear relationship in experiments, we simulated the mode shift varying with the refractive index, as shown in Figure S7 (red square). The linear fitting was then acquired：

$$Y=9.74\ n-13.82014\ (R^2=0.99)$$

where Y, n, and R^2 are mode shift, ZIF-8 refractive index, and correlation coefficient, respectively.

To illustrate, the refractive index of ZIF-8 after adsorbing 8000 ppm ethanol gas was estimated as follows:

According to first equation, the mode shift corresponding to 8000 ppm ethanol gas can be obtained：Y=0.32525 nm. And then, substituting this value into the simulation equation, the refractive index was determined to be: n=1.452 RIU.

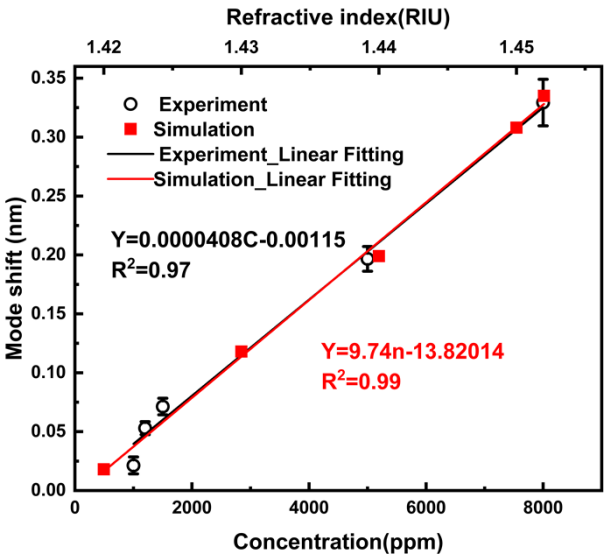

Figure S7. Experimental and simulated results of the mode shift in correlation with the varying concentrations of ethanol gas and ZIF-8 refractive index.

Calculation of LOD. The limit of detection (LOD) is given by: LOD = 3σ/S, where σ denotes the standard deviation and S represents the sensitivity. Generally, σ is the standard deviation of the blank sample (in the air environment) or the low concentration sample (1000 ppm).

1. Standard deviation of the blank (in the air environment)

We measured 10 sets (N = 10) of WGMs spectra of the sample in the **air environment** (0 ppm) and recorded the corresponding resonant peak position： 512.356 nm, 512.371 nm, 512.357 nm, 512.366 nm, 512.366 nm, 512.352 nm, 512.370 nm, 512.356 nm, 512.390 nm, 512.357 nm. Therefore, we have:

$$\sigma = \sqrt{\frac{1}{N}\sum_{i=1}^{N}(\lambda_i - \bar{\lambda})^2} = 0.010724 \text{ nm}$$

Where λ_i represents the i-th resonance wavelength, $\bar{\lambda}$ represents the mean of the measured resonance wavelength, N represents the total number of measured resonance wavelengths.

By combining the sensitivity in both experiments and simulations as shown in

Figure S7 (0.0408 pm/ppm and 9.74 nm/RIU, respectively), we have:

$$LOD = \frac{3\sigma}{S} = \frac{3 \times 0.010724}{0.0000408} = 789\ ppm$$

Likewise, based on RIU, we have：LOD=3.30×10^{-3} RIU ”

2. Standard deviation of the low concentration sample (1000 ppm).

Using the standard deviation of the blank sample is a simple and quick method. However, the weakness is that there is no objective evidence to prove that a low concentration of analyte will indeed produce a signal distinguishable from a sample blank (0 concentration). Therefore, we conducted additional experimental measurements to determine the lowest concentration that the sensor can resolve by decreasing it from 1000 ppm to 900 ppm, and the spectra are shown in Figure S8:

It is notable that there are tiny modes shifts when the concentration was set to 1000 ppm, while there is no visible variation on the mode shift when the concentration was down to 900 ppm. Therefore, we calculate the standard deviation of the lowest concentration sample (1000 ppm) to achieve the LOD.

Again, we measured 10 sets (N = 10) of WGMs spectra of the sample in the **ethanol environment** (1000 ppm) and recorded the corresponding resonant peak position：512.381 nm, 512.383 nm, 512.375 nm, 512.388 nm, 512.412 nm, 512.382 nm, 512.380 nm, 512.395 nm, 512.403 nm, 512.375 nm. Therefore, we have:

$$\sigma = \sqrt{\frac{1}{N}\sum_{i=1}^{N}(\lambda_i - \bar{\lambda})^2} \text{ =0.011655 nm}$$

Where λ_i represents the i-th resonance wavelength, $\bar{\lambda}$ represents the mean of the measured resonance wavelength, N represents the total number of measured resonance wavelengths.

By combining the sensitivity in both experiments and simulations as shown in Figure S7 (0.0408 pm/ppm and 9.74 nm/RIU, respectively), we have:

$$LOD = \frac{3\sigma}{S} = \frac{3 \times 0.011655}{0.0000408} = 857\ ppm$$

Likewise, based on RIU, we have：LOD=3.59×10^{-3} RIU.

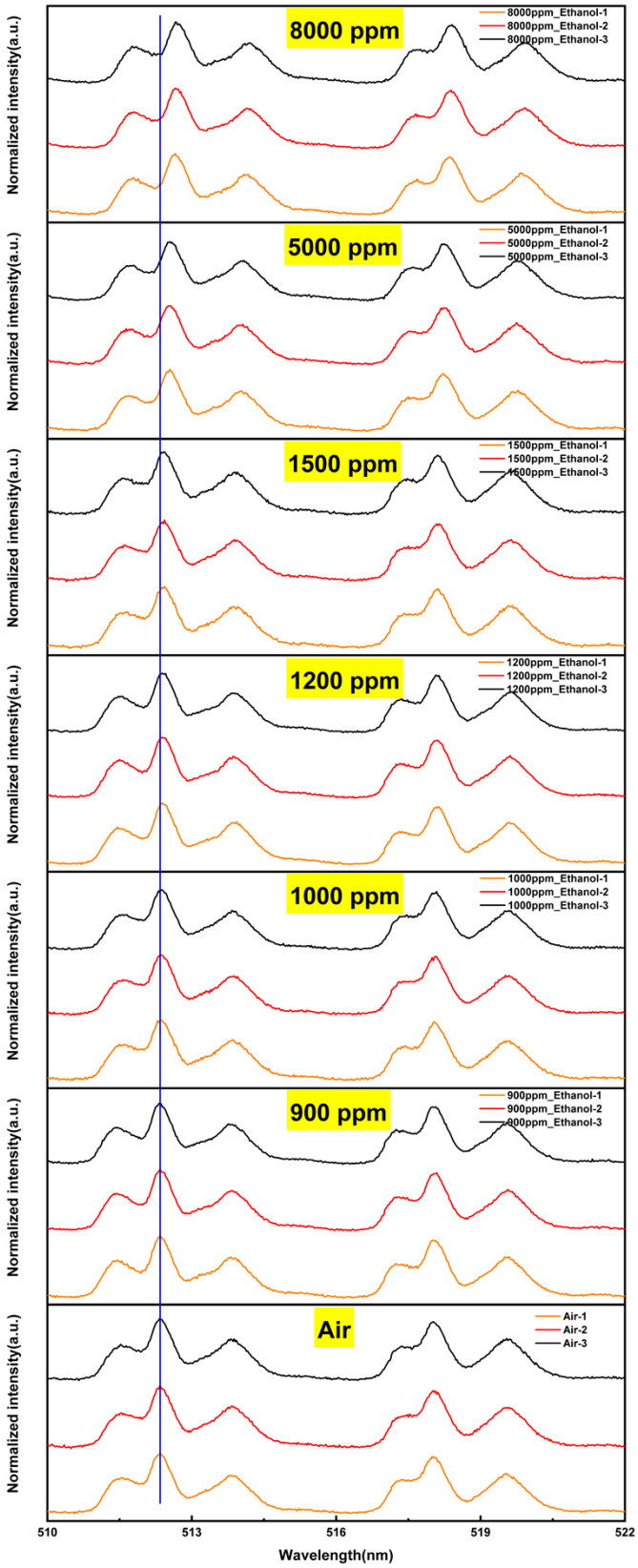

Figure S8. WGMs spectra of three replicate measurements of ZIF-8-nanoparticle decorated microsphere cavities at different ethanol gas concentrations

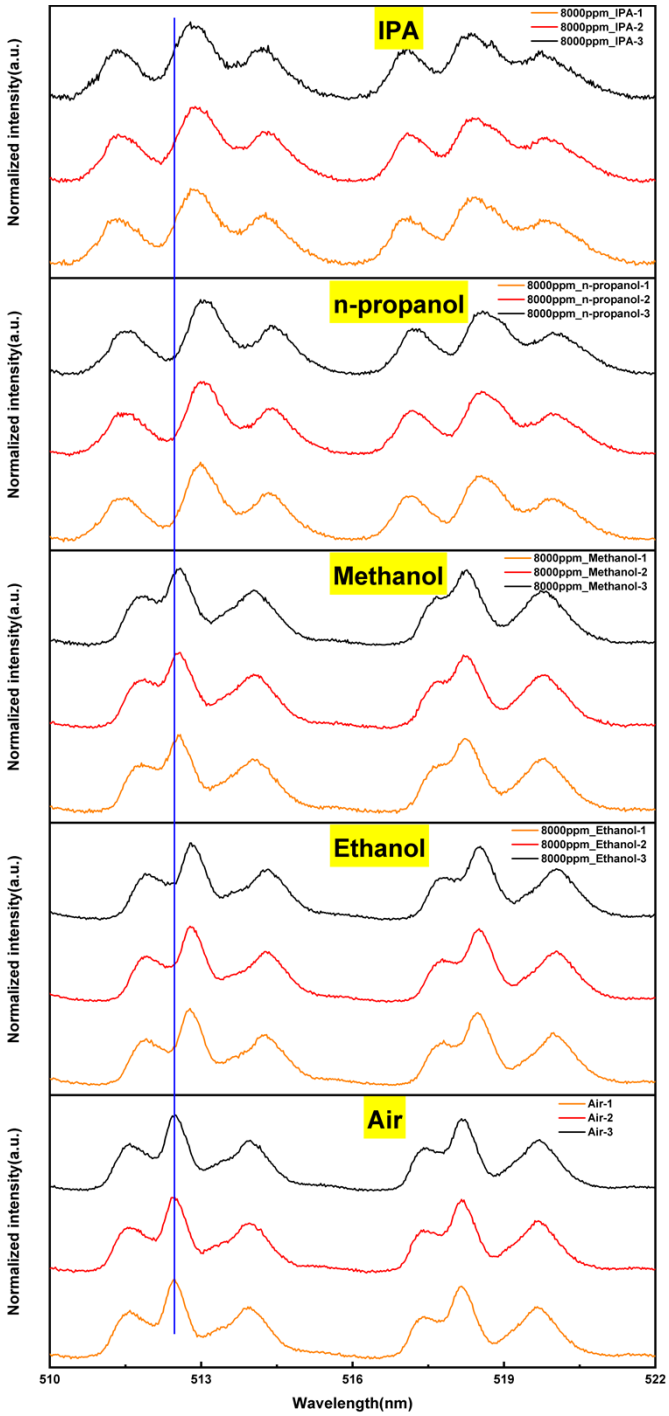

Figure S9. WGMs spectra of three replicate measurements of ZIF-8-nanoparticle decorated microsphere cavities under different VOCs gases at 8000ppm.

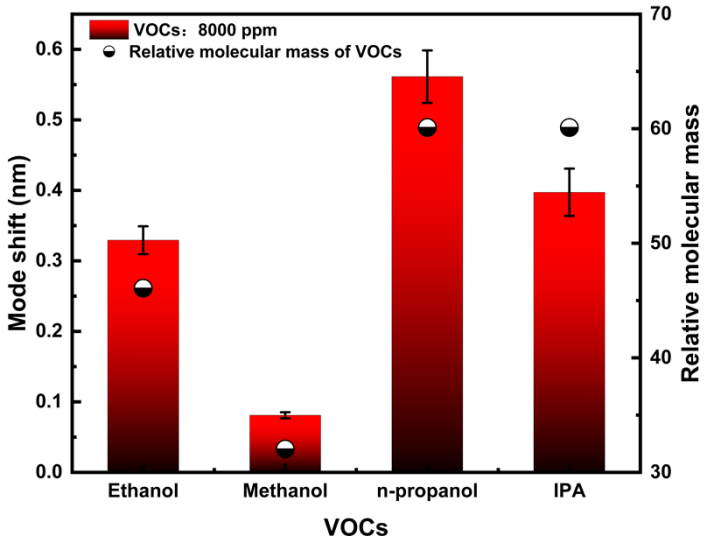

Figure S10. Statistical distribution of the mode shifts of ZIF-8-nanoparticle decorated microsphere cavities under different VOCs gases at 8000ppm

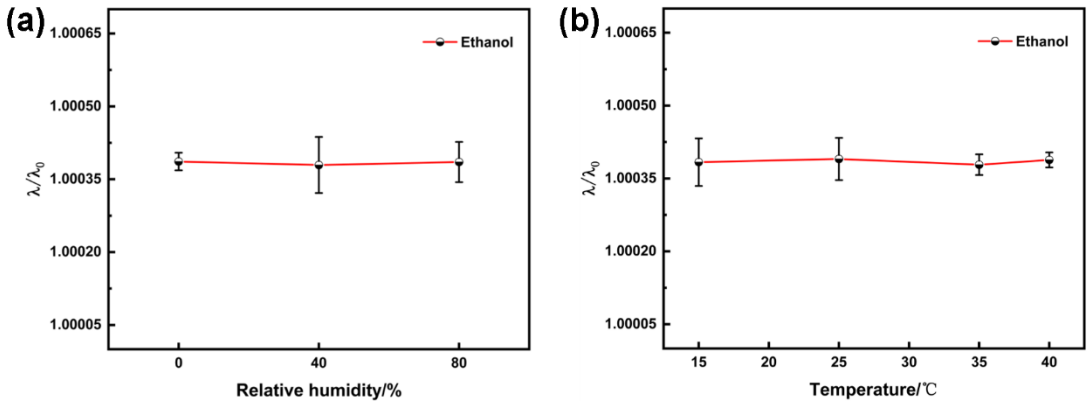

Figure S11. The response value of the ZIF-8-nanoparticle decorated microsphere cavities to 5000ppm ethanol gas varies with temperature and humidity

Table S1. Some different types of VOCs sensors and their sensing performance

Structure	Component for gas gathering	VOCs	LOD	Refs.
Fabry-Perot	SU-8 and PDMS	Acetone	2336 ppm	3
PDMS film	N/A	Ethanol	1500 ppm	4
Fabry-Perot	ZIF-8	Acetone	1000 ppm	5
Flat film	Polyhedral ZIF-8	n-Heptane	500 ppm	6
Ag nanotube	ZIF-8	Toluene	200 ppm	7
Flat film	$Co_3[Co(CN)_6]_2$	Ethanol	50-500 ppm	8

MoS_2/SiO_2 Microsphere	N/A	Ethanol	2.4×10^{-3} RIU	9
Microsphere	ZIF-8	Ethanol	3.30×10^{-3} RIU (789 ppm)	this work

IV. Theoretical calculation

The numerical simulation is based on the finite element method, to establish a two-dimensional theoretical model (Figure S12), set the PS microsphere cavity with a refractive index RI=1.6, load a 320 nm ZIF-8 nanoparticle layer on the surface of the microsphere, and the coating area is half a circumference. In order to ensure accuracy, the grid size of the structure is set to be less than 1/15 of the wavelength. The simulation is carried out in the electromagnetic wave frequency domain, and the resonance wavelength is obtained by calculating the eigenfrequencies of the structure (with perfect matched layers on the boundary)

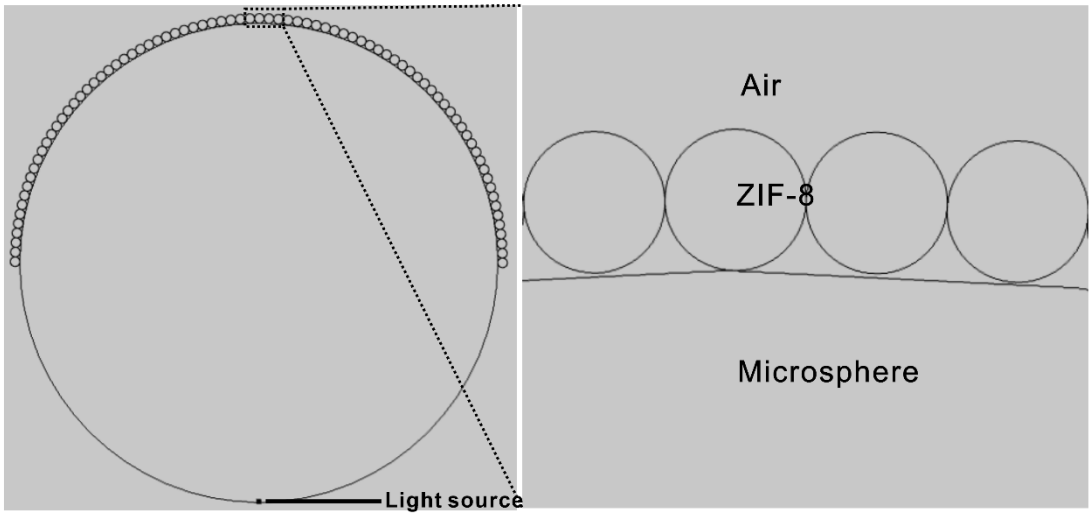

Figure S12. Two-dimensional theoretical model based on Finite Element Method.

V. Reference

[1]. L. Bai, Y. He, J. Zhou, Y. Lim, V. C. Mai, Y. Chen, S. Hou, Y. Zhao, J. Zhang and H. Duan, *Advanced Optical Materials*, 2019, 7,1900522.

[2]. D. T. Hallinan, M. Minelli, O. Oparaji, A. Sardano, O. Iyiola, A. R. Garcia and D. J. Burnett, Membranes, 2022, 12, 1059.

[3]. Reddy, K., Guo, Y., Liu, J., Lee, W., Oo, M. K. K., and Fan, X., *Sensors and Actuators B: Chemical*, 2011, *159*, 60-65.

[4]. C. Martínez-Hipatl, S. Muñoz-Aguirre, G. Beltrán-Pérez, J. Castillo-Mixcóatl and J. Rivera-De la Rosa, *Sensors and Actuators B: Chemical*, 2010, 147, 37-42.

[5]. C. Li, L. Li, S. Yu, X. Jiao and D. Chen, *Advanced Materials Technologies*, 2016, 1, 1600127.

[6] S. Yu, X. Wang, X. Jiao, C. Li and D. Chen, *Journal of Materials Chemistry C*, 2021, 9, 5379-5386.

[7]. C. S. L. Koh, H. K. Lee, X. Han, H. Y. F. Sim and X. Y. Ling, *Chemical Communications*, 2018, 54, 2546-2549.

[8]. Z. Wang and Q. Chen, *Spectrochimica Acta Part A: Molecular and Biomolecular Spectroscopy*, 2018, 194, 158-162.

[9]. Y. Mi, Z. Zhang, L. Zhao, S. Zhang, J. Chen, Q. Ji, J. Shi, X. Zhou, R. Wang, J. Shi, W. Du, Z. Wu, X. Qiu, Q. Zhang, Y. Zhang and X. Liu, *Small*, 2017, 13. 1701694.